

LoREA: A Backscatter Reader for Everyone!

Ambuj Varshney¹, Oliver Harms¹, Carlos Pérez-Penichet¹, Christian Rohner¹, Frederik Hermans¹, Thiemo Voigt^{1,2}
 {ambuj.varshney, carlos.penichet, christian.rohner, frederik.hermans, thiemo.voigt}@it.uu.se
¹Uppsala University, Sweden ²SICS Swedish ICT

ABSTRACT

Computational RFID (CRFID) platforms have enabled reconfigurable, battery-free applications for close to a decade. However, several factors have impeded their wide-spread adoption: low communication range, low throughput, and expensive infrastructure—CRFID readers usually cost upwards of \$1000.

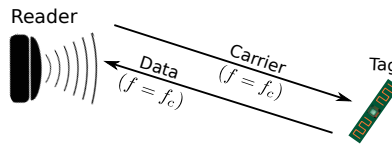
This paper presents LOREA, a backscatter reader that achieves an order of magnitude higher range than existing CRFID readers, while costing a fraction of their price. LOREA achieves this by diverging from existing designs of CRFID readers and more specifically, how self-interference is tackled. LOREA builds on recent work that frequency-shifts backscatter transmissions away from the carrier signal to reduce self-interference. LOREA also decouples the carrier generation from the reader, helping to further decrease self-interference. Decoupling carrier generation also enables the use of deployed infrastructure of smartphones and sensor nodes to provide the carrier signal. Together these methods reduce cost and complexity of the reader. LOREA also purposefully operates at lower bitrates than recent backscatter systems which enables high sensitivity and longer range.

We evaluate LOREA experimentally and find that it achieves a communication range of up to 225 m in line-of-sight scenarios. In indoor environments, where the signal traverses several walls separating the reader and the backscatter tag, LOREA achieves a range of 30 m. These results illustrate how LOREA outperforms state-of-art backscatter systems and CRFID platforms.

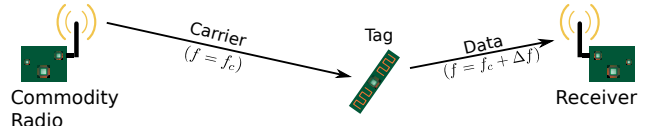
1. INTRODUCTION

Backscatter transmissions consume several orders of magnitude less energy than conventional radios, enabling devices which are both networked and battery-free [28, 31, 35, 29]. A backscatter transmitter modulates ambient radio signals by reflecting or absorbing them, which consumes less than 1 μ W of power [28], making backscatter well-suited for applications where replacing batteries is challenging [31, 56] or extending battery life is important [17].

Computational RFID (CRFID) tags, such as WISP [42] and Moo [60], are backscatter platforms that



(a) System based on a traditional reader.



(b) System based on the LOREA design.

Figure 1: *Comparison of LOREA with traditional backscatter systems.* LOREA decouples the carrier generator from the receiver, and uses commodity radios both to generate the carrier and receive the backscattered signals. LOREA avoids self-interference by frequency shifting the data away from the carrier.

augment traditional RFID tags with sensing and computing abilities [6]. CRFID tags often operate on harvested energy, and can operate in environments where only scarce amounts of energy are available for harvesting [57]. CRFID tags can drastically decrease the maintenance costs of sensing applications due to battery-free operations, as replacing batteries is often a costly and cumbersome endeavour [52]. CRFID platforms have enabled many novel applications like battery-free cameras [31], passive localisation using light [10], and activity detection [7]. But despite the numerous advantages and nearly a decade of research [42, 60], CRFID tags have seen only very limited adoption.

To understand the reasons for limited adoption of CRFID tags, we look at how these tags communicate in Figure 1(a). CRFID tags require an external device (reader) to generate a strong carrier signal to power, query the backscatter tag, and to receive

System name	LoRea	Passive WiFi [24]	HitchHike [61]	InterScatter [21]	BLE [11]	BackFi [3]	RFID [19]
Carrier strength (dBm)	26	30	30	20	15	30	31.5
Reported range (m)	225/175	33	54	10	9.5	5	>10
Bitrate (kbps)	2.9/197	1000/11000	222	1000/11000	1000	1000	640
Complexity	Low	Medium/High	Medium	Medium/High	Medium	High	High
Tag platform	MCUs	FPGA/ASIC	FPGA	FPGA/ASIC	FPGA	FPGA	ASIC

Table 1: Comparison of LOREA with recent backscatter systems. (LOREA’s backscatter tag was located at a distance of 1 m from the carrier generator, similar to all the other systems. Reported range are line-of-sight.)

the weak backscatter transmissions. Commonly, RFID readers or software defined radios (SDRs) are used as readers, which are often expensive (costing upwards of \$1000 [19]), bulky and consume large amounts of power. The CRFID readers and tags are also restricted by the protocol used EPC Gen 2 [12]. This protocol was designed to query small amounts of identification data on passive RFID tags, which makes it difficult to support data-intensive applications [15]. Furthermore, CRFID readers also demonstrate poor receiver sensitivity which limits the communication range and operations in through-the-wall environments. The disadvantages mentioned above severely restrict the applications conceived using CRFID platforms. While SDR-based readers can query CRFID tags, and achieve high throughput using custom protocols, using SDR-based readers only partially solves the problem. SDR-based readers increase the cost and complexity of deployments, while achieving communication ranges of only a few meters [16, 58, 54, 8].

Readers employed to query CRFID tags demonstrate poor performance and high cost primarily due to the need to tackle severe self-interference from the carrier signal [30, 17]. Existing CRFID readers receive backscatter transmissions at the same frequency as the carrier signal [16, 58, 54, 19, 8]. As energy delivery is combined together with communication, these readers generate a strong carrier signal (~ 30 dBm). The backscatter reflections, on the other hand, are weak hence separating them from the strong carrier requires complex techniques and components increasing the cost and the complexity of the reader [17]. Even with the additional complexity and cost to mitigate self-interference, CRFID readers still demonstrate poor receive sensitivity due to leakages of the carrier signal [30] achieving a range of only several meters.

This paper answers the question: *Can we redesign backscatter readers such that they overcome the limitations of low range, high complexity and high cost?* LOREA enables battery-free applications inconceivable on existing generation of CRFID tags and readers, and also paves way for widespread adoption.

Contributions. To address the challenge of existing backscatter readers, we design LOREA, a low-cost, low-power high-range, and low-complexity backscatter reader. LOREA achieves the above mentioned goals by diverging from existing designs of CRFID tags and read-

ers in three important ways:

1. LOREA builds on recent systems [24, 30, 59] that separate the carrier from the backscatter transmissions as shown in Figure 1(b). In this way, the carrier and the transmissions do not overlap which avoids self-interference, and the need for the kind of complex solutions that existing backscatter readers employ. To reduce self-interference, we simply leverage the ability to reject emissions on adjacent channels which is present in commodity RF transceivers. Furthermore, this approach also improves the SNR of the backscatter signal as it is less interfered from the carrier (see Section 2).
2. LOREA deliberately operates at bitrates much lower than used in recent backscatter systems [24, 21, 61] and RFID readers. As receiver sensitivity improves with lower bitrates, LOREA is capable of significantly higher ranges when compared to recent backscatter systems (see also Table 1). Lower bitrates also enable the generation of the modulating signal on MCU-based CRFID platforms.
3. Finally, LOREA decouples the carrier generator and the receiver in space, and uses the 2.4 GHz ISM band for transmissions. This design choice enables the use of existing infrastructure composed of sensor nodes [36], smartphones [21], or SDRs to generate the carrier signals. The spatial decoupling also helps to decrease self-interference due to the distance between the receiver and the carrier generator. Decoupling the energy-expensive carrier generation from the reader also significantly decreases the power consumption.

The above contributions together make LOREA achieve the following: First, a cost of about \$70 using off-the-shelf components, whereas the cost of a conventional RFID reader is \$500–\$2000. Second, a range beyond 200 m in line of sight. This is an order of magnitude higher than with traditional RFID readers, seven times higher than the reported range of Passive WiFi [24], and four times higher than the reported range of HitchHike [61], two recent backscatter systems (see also Table 1).

We illustrate two representative use cases that demonstrate LOREA’s capabilities: First, we present a system that uses visible light to passively detect the presence of a person. While similar system suffered from short range, the LoRea-based system allows the reader

to be placed in another room and yet report events with high accuracy. In the second use case, we demonstrate that LOREA’s low-power mode and decoupling of the carrier enables mobile readers even in non-line-of-sight environments achieving high range.

Note that in our use cases, as well as in the rest of the paper, we focus on the uplink from the backscatter tag to the reader since most sensing applications are bottlenecked by this link [3, 61]. We can support downlink communication by reusing existing low-power receiver designs [21, 23]. Existing CRFID readers also couple together energy delivery with communication, which has been shown to be inefficient [14, 57, 40]. We hence decouple the energy delivery from the reader. LOREA, if needed, can support RF-based energy harvesting by reusing design of energy harvester presented by Talla et al. [44], or by using other harvesting methods [5].

2. BACKGROUND

RFID readers. Radio-frequency identification (RFID) reader queries backscatters tags for their identification data (ID) as shown in Figure 1(a). In the case of passive tags, the reader also provides energy to the tags and hence sends a strong carrier signal.

In existing systems, the RFID tags backscatter ID data at the same frequency as the carrier, and hence must employ sophisticated mechanisms to reduce self-interference and recover the weak backscatter signal. These mechanisms usually are a combination of methods that: Isolate the carrier from the receiver using circulators, employ RF cancellation to attenuate the self-interfering signal and attempt to separate the self-interference signal [17]. All these methods cause additional power consumption and increase the complexity and cost of the reader. For example, Impinj’s R2000 RFID chip consumes an additional 500 mW of power when self jammer cancellation is turned on [20]. Furthermore, the use of circulators comes with an insertion loss penalty causing a reduction in received signal strength and the need to increase the output power to achieve the same level of radiated signal, which in turn is detrimental to the receiver and limits the achievable range. Conventional RFID readers are also usually used in CRFID applications

SDR-based readers have also been used to query CRFID tags. These readers do not include any specialized hardware to reduce self-interference from the strong carrier, instead they resort to operating in a bistatic configuration [8]. SDR-based readers owing to lack of self-interference cancellation mechanisms demonstrate a range of only a few meters [16, 58, 54].

Backscatter communication primer. Radio Frequency (RF) signals are absorbed or reflected by different amounts by an antenna, dictated by the radar cross section (RCS) of the antenna. The RCS of an antenna is controlled by changing the impedance of the circuit connected to the antenna. Backscatter transmitters mod-

ulate their RCS to control the degree of absorption or reflection of impinging ambient RF signals. The act of reflection or absorption produces weak variations of the ambient signal which can be decoded by a receiver.

Consider an RF emitter transmitting a signal that reaches a backscatter transmitter which, in turn, selectively reflects or absorbs the signal. A receiver observes these signals. The signal $R(t)$ perceived by the receiver consists of two components: One directly coming from the emitter $S_{rt}(t)$. Another coming from the backscatter device $B(t)S_{bt}(t)$, which is the minute variations generated according to transmit data. The resulting signal, as observed by the receiver is:

$$R(t) = S_{rt}(t) + \sigma B(t)S_{bt}(t) \quad (1)$$

In the above equation, σ is the RCS of the device and $B(t)$ is either 0 or 1 and represents whether the backscatter device is absorbing or reflecting the ambient signal. In traditional CRFID readers, the reader generates a constant tone signal or a sinusoid at frequency f_c , and the backscatter tag also backscatters at the same frequency, i.e., in the above equation both components are at same frequency. The reader is also responsible for both generating the carrier and observing the backscattered signal from the tag.

Backscatter as mixing process. As stated above in Equation (1), the backscattered signal from the transmitter is proportional to the product of the data signal $B(t)$ and the ambient RF signal reaching the backscatter transmitters antenna $S_{bt}(t)$. Backscatter readers generate a single-tone sinusoidal wave of frequency f_c as a carrier signal. If we consider this signal reaching the backscatter transmitter while the RCS of the backscatter antenna is changed at a frequency Δf , the resulting backscattered signal (product $\sigma B(t)S_{bt}(t)$ in Equation 1) takes the form:

$$2 \sin(f_c t) \sin(\Delta f t) = \cos[(f_c + \Delta f)t] - \cos[(f_c - \Delta f)t]. \quad (2)$$

We observe, the product of the backscattered signal with impinging radio signal can be expanded into two images of the original signal, modulated by the backscattered data. The images are frequency-displaced by an amount equal to Δf on both sides of the original signal’s centre frequency. This displacement allows the backscatter tag to shift the backscattered signal away from the carrier, and also allows the receiver to reduce interference from the carrier signal [24, 61, 37, 36].

3. DESIGN

In this section, we present the design of LOREA. We also compare LOREA’s power consumption and cost to that of conventional RFID readers.

3.1 Decoupling in Frequency and Space

One of the main differences between LOREA and conventional CRFID readers is the way in which they tackle

self-interference. Reducing self-interference is important since otherwise the strong carrier overwhelms the backscattered signal that is inherently weak [17]. To reduce self-interference we make three main design choices which diverge from conventional CRFID systems.

First, LOREA uses *different frequencies* for the carrier wave and the backscattered signal. As opposed to conventional CRFID readers, where the carrier wave is at the same frequency as the backscattered signal, we instead deliberately place the carrier an offset Δf away from the operating frequency of the reader. Existing low-power radios like the ones used for WiFi [24, 21], ZigBee [21, 37, 36], Bluetooth [11, 21] or other ISM band transceivers demonstrate the ability to greatly attenuate signals present in the adjacent frequency bands. For example, the CC2500 attenuates a signal present 2 MHz away from the tuned frequency by almost 50 dB (Figure 2). We leverage this ability to significantly attenuate the strong carrier signal, thus reducing self-interference without using complex components or techniques employed on existing readers.

Second, as opposed to existing CRFID tags that backscatter at the baseband frequencies [55, 30], LOREA instead *backscatters on an intermediate frequency*. We leverage the mixing process inherent to backscatter transmissions to both modulate the carrier, and also to shift the modulated signal to the desired frequency $f_r = f_c + \Delta f$ on which the receiver listens for transmissions. This helps to receive information, while the carrier being backscattered is located some frequency offset away from receivers frequency.

Finally, LOREA *decouples carrier generation and reception spatially*. Spatial separation reduces self-interference significantly due to propagation loss of the carrier signal [8]. On existing RFID readers the carrier generator and the receivers are co-located and have to employ complex components like circulators to reduce self-interference and to improve the noise floor. Besides interference reduction, the separation also enables the use of existing infrastructure, such as sensor nodes and smartphones, to generate the carrier signal. This can improve the scalability of the system, for example.

These three design choices lead to our reader architecture shown in Figure 1(b). Rather than having one single reader device, the reader’s functionality is split into carrier generation and reception. We discuss these in more detail in the next section.

3.2 Receiver

The receiver’s task is to receive and decode tags’ backscattered transmissions. The decoupling of the carrier generator and receiver in both frequency and space opens a design space for choosing a transceiver, selecting the frequency offset as well as the modulation scheme. We detail these aspects in the following:

Transceiver. On the LOREA reader we use radio transceivers that support only basic link-layer functionalities without supporting higher layer protocol stacks

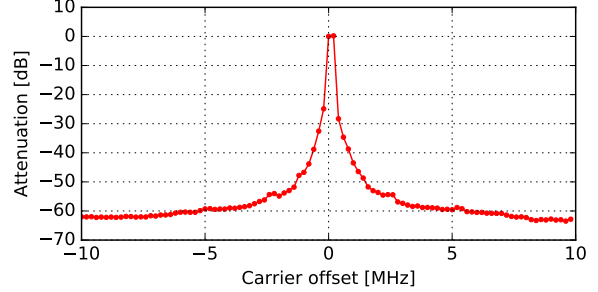


Figure 2: *Carrier interference rejection.* The transceiver used in LOREA reduces interference from a carrier located 2 MHz away by almost 50 dB.

like ZigBee, WiFi or BLE. This is done in order to achieve high range, enable maximum configurability and achieve low power. This particular design choice has two major implications.

First, these transceivers support modulation schemes such as On-Off-Keying (OOK) and Frequency-Shift-Keying (FSK). The low complexity of these modulation schemes enables easy generation of the baseband signals on the backscatter tag. Second, these radios support lower bit rates (2.9 kbps), which improves the receiver sensitivity by almost 10 dB to 15 dB as compared to operating at higher bitrates of $\sim 100\text{-}500$ kbps. This significantly increases communication range and improves the ability to operate in non line of sight environments. As most sensing applications send only a small amount of data to the receiver [34] these applications can benefit from the high bitrates – a low bitrate is, however, not detrimental to their performance. To support other applications requiring high bitrates, we can also operate the reader at high bitrates with reduced sensitivity.

Our implementation of LOREA uses the Texas Instruments CC2500 [47].

Selecting Frequency Offset. In LOREA, the carrier and backscatter signal are separated in frequency. The frequency offset Δf corresponding to this separation needs to be high enough to reduce self-interference from the carrier signal, and at the same time, small enough so that it can be generated on commodity MCUs on a low power backscatter tag.

We conduct an experiment to determine Δf needed for the LOREA reader: We setup a software defined radio (SDR), and position its antenna about 30 cm away from the antenna of our CC2500-based receiver. We program the SDR to generate an unmodulated carrier signal of strength 12 dBm which is maximum that could be generated from our SDR, and tune the frequency of the carrier to be at the receiver’s centre frequency f . We program the receiver to measure the noise floor repeatedly. When the carrier is at the receiver’s center frequency, the noise floor is significantly high owing to significant self-interference. Next, we program the SDR to slowly sweep the frequency of the carrier in steps of

250 kHz at intervals of 60 seconds, until it reaches a frequency $f - 10$ MHz on the negative side, and a frequency $f + 10$ MHz on the positive side of the spectrum. We find the mean noise floor at different offsets of the carrier, and find the change in noise floor from the levels when the carrier was present at f .

Figure 2 demonstrates the result. The noise floor improves by almost 50 dB as the carrier is shifted 2 MHz away from f_c but does not improve significantly further away. Hence, we consider $\Delta f = 2$ MHz as a good trade-off for our implementation.

Selecting Modulation Scheme. Using an off-the-shelf radio transceiver as a receiver opens the possibility of letting the applications dictate the choice of modulation scheme employed. While the available choices are somewhat limited if the baseband signal has to be generated by a commodity MCU, selecting among simpler modulation schemes such as OOK and FSK is possible.

CRFID tags usually employ some variant of amplitude modulation (OOK/ASK) since they use the same modulation scheme for receptions. They achieve energy-efficient receptions with a simple envelope detector that is based on amplitude modulation [28].

As we focus on upstream communication from tags to the reader, LOREA is not constrained to amplitude modulation, but our tags can use FSK for upstream communication which yields the following advantages: First, FSK is a constant envelope modulation [39] and as such offers a number of advantages for the receiver, in particular the robustness against fading. Second, FSK is more energy-efficient than OOK in the sense that it can achieve a lower Bit error rate (BER) for the same signal-to-noise ratio [25, 39].

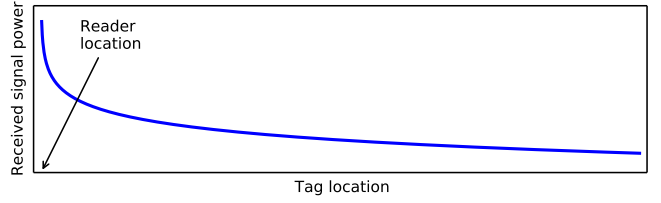
3.3 Carrier Generation

Monostatic vs. bistatic setups. To transmit data, backscatter tags require an unmodulated carrier wave that they can modulate. Most existing RFID systems follow a *monostatic* setup, in which the RFID reader uses the same antenna for emitting a suitable carrier and for receiving transmissions from backscatter tags [25, 33]. An advantage with this setup is its conceptual simplicity. However, monostatic setups require the RFID reader to perform complex self-interference cancellation, because the emitted carrier is much stronger than the signals from the backscatter tags. Circulators are used to reduce self-interference, but they increase the readers' cost, and still affect receive sensitivity due to leakages of the carrier signal [30].

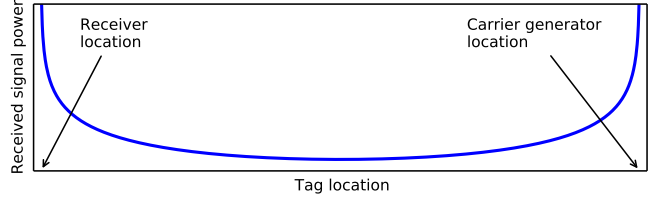
Monostatic configurations also limit the communication range. Consider the strength P_r of a backscattered signal at the reader in free space [24, 33], given by

$$P_r = \left(\frac{P_t G_t}{4\pi d_1^2} \right) K \left(\frac{\lambda^2 G_r}{4\pi d_2^2 4\pi} \right).$$

Here, λ is the carrier's wave length, P_t is the power of the carrier, and the factor K accounts for the return



(a) Signal strength in monostatic setup, as the tag's distance to the reader increases.



(b) Signal strength in bistatic setup, as the tag is placed on a straight line between receiver and carrier generator.

Figure 3: *Signal strength for monostatic and bistatic setups.* LOREA's bistatic setup increases the communication range, as there are more locations from which a signal can be backscattered with a high signal strength.

loss and antenna gains at the backscatter tag. G_t and G_r represent the antenna gain for transmitting the carrier and receiving the backscattered signal, respectively. Similarly, d_1 denotes the distance of the backscatter tag to the carrier generator and d_2 denotes the distance of the tag to the receiver. Thus, in a monostatic configuration, $d_1 = d_2$ and $G_t = G_r$. Fig. 3(a) plots the received power using the above equation, assuming a monostatic configuration. As expected, minimizing the distance to the RFID reader maximizes the received signal strength.

In contrast, LOREA uses a *bistatic* configuration, in which receiver and carrier generator do not share the same antenna and can be spatially separated. This means that for LOREA d_1 does not need to be identical to d_2 . Therefore, the received signal strength will be high as long as a backscatter tag is located in proximity to either the receiver or the backscatter tag. This allows to increase the communication range of a backscatter system. Based on the above equation, Fig. 3(b) shows the signal strength as a tag is moved on the straight line between a reader and a carrier generator.

Another advantage of using a bistatic configuration is that the receiver does not need to handle interference from the carrier generator, provided that both are sufficiently separated in space. This reduces the cost and complexity of a LOREA reader.

Generating carriers. LOREA can leverage a range of devices to generate suitable carrier waves. For example, high-power carrier waves can be easily generated using software-defined radios, in particular in combination with amplifiers. Furthermore, many radio transceivers provide a test mode for FCC compliance testing that generates an unmodulated carrier. In Sec. 4, we use

Component	CC2420	CC3200	CC2500	Beaglebone	MSP430	Frontend	RFID Reader
Task	Carrier generator	Receiver		Backscatter tag			RFID Reader
Power (mW)	52	687	39.9-58.8	10.9	7.2	0.0003	11500-15000
Cost (\$)	11.1	29	5.0	45	16	1	1585.0

Table 2: Power consumption and cost of LOREA’s components in comparison with RFID Reader

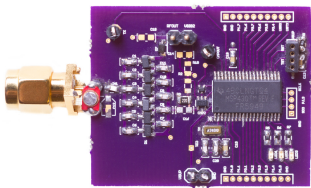


Figure 4: *MSP430 based backscatter tag.*

TelosB sensor nodes that feature a CC2420 radio chip, and WiFi radio CC3200 to generate an unmodulated carrier wave. Recent work has also shown how carriers may be generated on smartphones using BLE radios [21]. Since a carrier wave does not contain any information, the generation of carriers does not need to be coordinated in a deployment. Indeed, LOREA can use any combination of carrier generators.

Carrier frequency. LOREA also differs from conventional RFID systems in that it operates in the 2.4 GHz ISM band. A key motivation for this decision is the world-wide availability of the 2.4 GHz band and its relatively high permissible transmit power. For example, in Europe only ~ 5 MHz of ISM band is available at 863-868 MHz as opposed to ~ 26 MHz in the US. We also opted for the 2.4 GHz ISM band as it allows us to leverage commodity radio transceivers for carrier generation, as described in the previous paragraph. Sub GHz frequencies offer better propagation characteristics and hence support longer ranges. LOREA can be optimised to use sub GHz radio transceivers [46] supporting similar modulation schemes and packet formats which would make them capable of operating at significantly lower receive sensitivity to achieve larger communication ranges. Our focus in this paper is to leverage existing deployed devices like smartphones and sensor nodes to provide a carrier signal. We leave a more detailed study of operating LOREA at lower frequencies to future work.

3.4 Backscatter Tag

At its core, a backscatter tag consists of two components: a radio front-end whose radar cross-section is controlled by a switch as outlined in Sec. 2; and a device that generates an appropriate baseband signal. This signal is then used to control the switch.

Backscatter front-end. Our front-end uses the Analog Devices HMC190BMS8 RF switch [1] that also recent backscatter systems employ [21, 24]. We design a

PCB on a two-layer FR4 substrate. We have measured the return loss of our front-end to be 3 dB, which is similar to recent designs [21, 24]. Backscatter transmissions have a side effect of creating an undesired mirror signal (see Eq. 2). Our present font-end does not remove this image. In the future, we will incorporate the design presented by Zhang et al. [61] to resolve this. Our backscatter frontend consumes $0.3 \mu\text{W}$ of power.

Generating baseband signals. To offset the backscattered signal from the carrier, we shift the baseband signal to the intermediate frequency of 2 MHz. The modulation scheme of choice is 2-FSK with a frequency deviation of ± 95 kHz, resulting in a reasonably narrow baseband signal that can be implemented in software. This means that to transmit a 1-bit, the tag generates a signal with a period of 477 ns for one symbol duration. To transmit a 0-bit, the tag generates a signal with a period of 525 ns instead.

We implement two prototype backscatter tags. The first prototype is based on the Beaglebone Black embedded platform [2] ($\sim \$45$). We use the Beaglebone’s programmable real-time unit (PRU) to generate the signal for a payload. The signal is generated by simply inserting appropriate delays between toggling the switch. We use the PRU instead of the Beaglebone’s main CPU to avoid interruptions from the operating system’s scheduler. The other prototype tag is based on the MSP430 FR5969 MCU [45] that is also used on present CRFID platforms [55]. We leverage the MCU’s on-board timers to generate the signal, which makes it possible to operate in low-power mode during most of the transmission. We instantiate two different MSP430-based tags: the first is our custom implementation shown in Fig. 4 and the other uses an off-the-shelf Texas Instrument launchpad board ($\$16$).

3.5 Power Consumption and Cost

Table 2 compares the power consumption of LOREA’s components to that of a commercial RFID reader, the Speedway Revolution R420 from Impinj [19]. For the carrier generators, we take the power consumption when the radio is actively transmitting at the highest output power and the CPU is active. For the receiver, we consider the power consumed when the CPU is active and the radio is receiving. The table shows that the power consumption of these components is at least an order of magnitude lower than that of a commercial reader. The same is true for the price where commercial readers often cost above \$1000 while the components we require for LOREA are significantly cheaper. Even though the

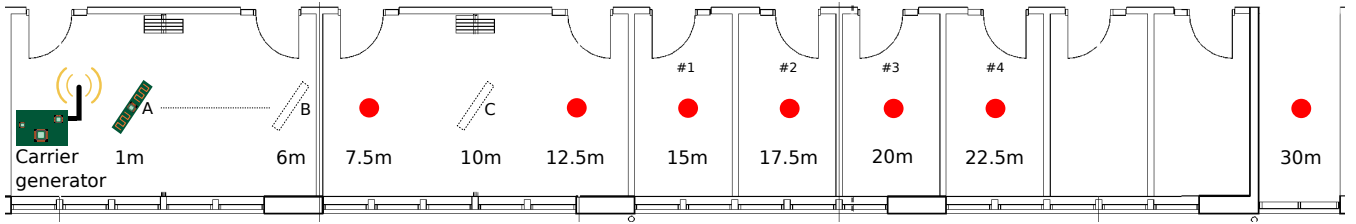


Figure 5: *Layout for the indoor experiments.* The carrier generator is placed in the first room, while we vary backscatter tag (A,B,C) and receiver (red dot) locations.

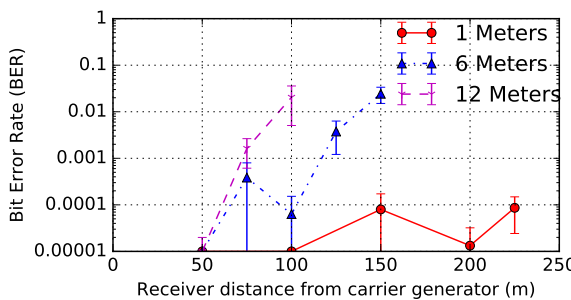


Figure 6: *Backscatter tag close to the carrier generator (outdoors).* Positioning the backscatter tag close to the carrier generator leads to a high range. A distance of 12 m is sufficient to achieve 100 m range at a BER of 10^{-2} .

focus of the paper is not on backscatter tags, for completeness we also show the power consumption of the prototype backscatter tags. We note, similar to recent works which generate passive wireless transmissions [24, 21] our tags need to generate only digital signals with a much simpler modulation scheme and at lower frequencies. Hence, we expect an IC implementation of our backscatter tag to consume similar amount (if not less) of power as compared to recent backscatter systems $\sim 10\text{-}50 \mu\text{W}$.

4. EVALUATION

This section presents the experimental results we collect to evaluate LOREA in different environments. Our results show that:

- In an outdoor setting, LOREA achieves one order of magnitude longer range than conventional RFID readers and CRFID tags.
- In an indoors environment, LOREA enables communication through multiple walls over distances of tens of meters.
- LOREA can make use of deployed infrastructure of ZigBee and WiFi radios to generate suitable carrier signals.

4.1 Range and Bit Error Rate

We first aim to understand the achievable range and

reliability of LOREA in different environments and operating modes.

Experimental setup. We equip both the carrier generator and the backscatter tag with an omni-directional antenna from TP-Link [50]. At the receiver, we use an onboard inverted-F antenna. To account for different antenna orientations and multi-path fading, we perform three independent runs of each experiment with random receiver antenna orientations.

Unless otherwise stated, we use our BeagleBone-based backscatter tags as transmitters. We generate a carrier signal with a strength of 26 dBm using a USRP B200 software defined radio [13] equipped with external amplifier. We note that our carrier signal is still four dB lower than the maximum permissible under FCC regulation, and that used by Passive WiFi [24] and Hitch-Hike [61]. We expect the range to further improve with higher carrier strengths.

We position the backscatter tag, receiver and carrier generator approximately one meter above the ground in all our experiments.

Metrics and communication parameters. In each experiment run, we transmit 100 randomly-generated packets of 64 bytes. On the receiver, we keep track of the received packet sequence number, signal strength and the noise floor. We collect approximately 10^5 bits, and compare the received bits with the transmitted bits as done in recent backscatter works [3, 59]. We calculate the bit error rate (BER) for each run of the experiment, along with its mean and standard deviation between experiments runs. Unless otherwise stated, the backscatter tags transmit at a rate of 2.9 kbps.

4.1.1 Outdoors

We begin our evaluation in outdoor environments with line-of-sight propagation. The experiments are carried out outside of our university, with buildings on one side and forest on the other side.

We first evaluate LOREA with the objective of assessing the impact of positioning the backscatter tag close to the carrier generator. Figure 6 shows the observed BER as a function of distance between the receiver and the carrier generator. We achieve a range of 225 m, 140 m, and 90 m with a separation of 1 m, 6 m, and 12 m from the carrier generator, respectively. In most cases, the BER is well below 10^{-2} . As the backscatter tag moves

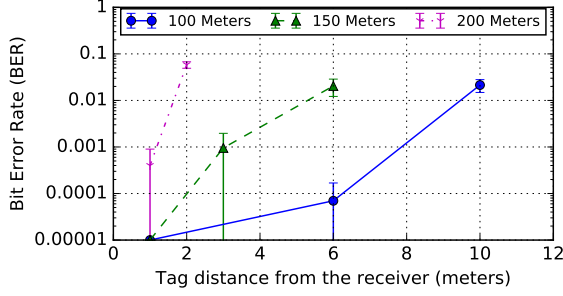


Figure 7: *Backscatter tag close to the receiver (outdoors)*. As the distance from the carrier generator increases, the maximum achievable range between the backscatter tag and the reader decreases.

away from the carrier generator, the achievable range decreases while the bit errors increase.

We next evaluate the impact of positioning the backscatter tag close to the reader. Figure 7 shows the result of the experiment. As both the backscatter tag and the reader move farther away from the carrier generator, the communication range decreases. When the backscatter tag is at a distance of 200 m, the reader can only receive reliably up to 2 m from the tag. However, as we move the backscatter tag close to the carrier generator at a distance of 100 m, we can receive reliably up to a distance of 10 m from the tag.

The results of the experiment suggest that the optimal position to achieve low BER and high range is to either position the backscatter tag close to the carrier generator, or to take the reader close to the backscatter tag, especially when operating at longer distances from the carrier generator. These results confirm the earlier findings in Figure 3(b).

Commodity radio based carrier generators. We also perform an experiment where we use a TI CC3200 Launchpad [48] (WiFi, \$30) and a TELOS B sensor node (802.15.4, \$70) as carrier generators. The tag is located 1 m from the carrier generator. With the WiFi-based platform, we achieve a range of 54 m, with the sensor node a range of 7.5 m. Both platforms feature only an on-board antenna with limited gain which limits the achievable range.

4.1.2 Indoors

Next, we evaluate the ability of LOREA to operate in non-line-of-sight environments. We perform experiments in an indoor environment in the presence of rich fading and other wireless networks. The environment is shown in Figure 5. The study rooms are of varying size between 2.5 m and 7.5 m, and each room is separated by an insulated gypsum wall of approximately 16 cm. The rooms are equipped with tables, chairs, and a whiteboard on the wall separating the rooms.

In a first experiment, we keep both the backscatter tag and the carrier generator in the same room (see

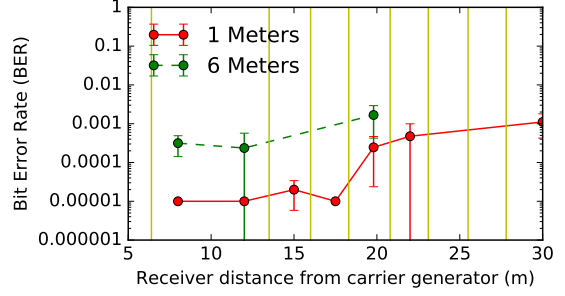


Figure 8: *Through the wall evaluation* The vertical lines indicate the presence of walls. When the backscatter tag is kept 1m from the carrier generator, we can receive transmissions at a BER of 10^{-3} eight wall aways at a distance 30 m from the carrier generator.

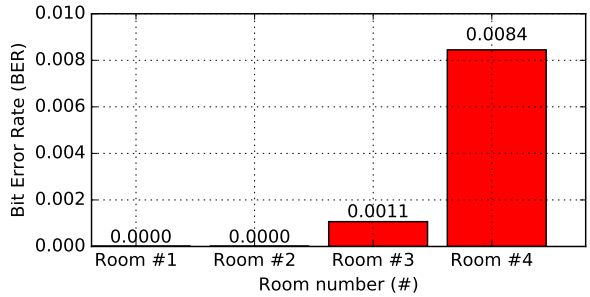


Figure 9: *Room to room backscatter*. Carrier generator and backscatter tag are placed in separate rooms and are separated by 10 m (tag position C). We can receive transmissions even four room away from the tag.

Figure 5). We position the backscatter tag 1 m, and 6 m away from the carrier generator. We vary the position of the LOREA receiver by placing it in different rooms.

Figure 8 shows the results, where vertical lines indicate the presence of walls in the figure. When the backscatter tag is located at a distance of 1 m from the carrier generator, we can achieve a distance of approximately 30 m between the LOREA receiver and carrier generator, traversing through eight walls. At longer distances the SNR falls below the sensitivity levels of the radio. As the distance between the backscatter tag and the carrier generator increases to 6 m, the strength of the backscatter signal reduces, which affects the achieved range and also introduces higher bit errors. We achieve a range of approximately 20 m with five walls separating backscatter tag and the receiver.

Room to Room Backscatter. We next evaluate LOREA in a scenario where backscatter tag, carrier generator and the receiver are all located in separate rooms. We keep the carrier generator in the same location as in the earlier experiment, and move the backscatter tag to the next room (tag position C). The distance between the backscatter tag and the carrier generator is 10 m,

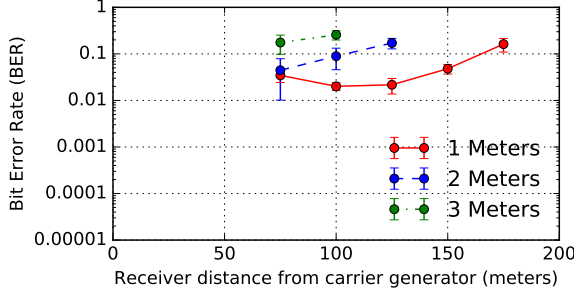


Figure 10: *High bitrate (197 kbps) with tag close to the carrier generator (outdoors).* A High bitrate reduces the achievable range and introduces higher bit errors as opposed to operating the reader at lower bitrates.

and a wall separates them. We place the receiver in different rooms and repeat the experiment.

Figure 9 shows the result of the experiment. We can receive backscattered transmissions four rooms away from the backscatter tag with four walls separating the backscatter tag and the receiver at BER lower than 10^{-2} . We note that existing CRFID systems do not operate well in through the wall scenarios [35]. Hence, we believe that LoREA’s ability to perform well in through the wall scenarios is a significant improvement.

4.1.3 High-speed Mode

Some sensing applications for CRFID platforms, such as battery-free cameras [31] or microphones [49], suffer from the low bitrates of CRFID. To support such applications, LoREA supports higher bitrates at the cost of reduced receiver sensitivity. We next perform an experiment to investigate this trade-off. We program the reader and the receiver to operate at a bitrate of 197 kbps, which is close to maximum achieved goodput [53] for ZigBee(802.15.4) widely used protocol to network sensors. The bitrate also gives us good sensitivity and high communication range.

We position the backscatter tag close to the carrier generator at distances of 1 m, 2 m and 3 m, and position the reader at intervals of 25 m starting at a distance of 75 m from the carrier generator. Figure 10 shows the result of the experiment. While we achieve a range of 100 m at a target BER of 10^{-2} when the backscatter tag is located 1 m apart from carrier generator, the observed BER increases significantly at larger distances.

The observed BER is significantly higher than at low bitrates at similar distances. However, the BER we achieve is comparable to the recent backscatter systems operating at similar bitrates, while we get a nearly threefold improvement in range [61]. The experiment suggests that high-speed mode should only be used at short distances or together with suitable mechanisms at the reader to recover lost or corrupt bits.

4.2 Goodput of LoREA and CRFID

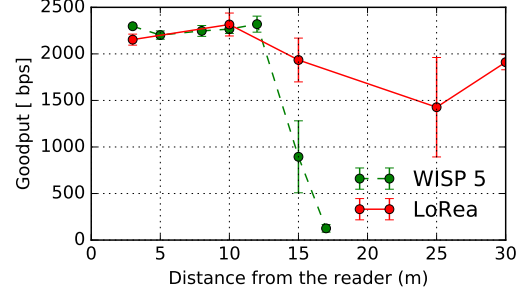


Figure 11: *Goodput comparison between WISP 5 and LoREA (outdoors).* WISP achieves a maximum range of only 18 meters.

In this experiment we compare the performance of LoREA to CRFID tags queried using a commercial RFID reader. We perform the experiment to understand improvements in terms of communication range.

Settings and metrics. We perform the experiment outdoors in settings similar to Section 4.1.1. We use the Wireless Identification and Sensing Platform (WISP) as the CRFID platform. WISP has been widely used [31, 55, 43] and developed for close to a decade [43]. We use the present generation, and the state-of-the-art WISP 5.0 for the experiments [55]. To query the WISP tags, we use a commercial RFID reader (Impinj Speedway R420 [19], $\sim \$1600$) equipped with a single 9 dBiC circular polarized antenna. We configure the reader to generate a carrier signal of strength 26 dBm, similar to the carrier strength used to evaluate the LoREA reader. We position the antenna and the WISP tags approximately one meter above the ground. As CRFID tags demonstrate an asymmetry in the communication and energy harvesting range [14], we externally power the WISP tags to avoid being restricted by the energy harvesting range. In the same setting, to evaluate LoREA, we connect a 9 dBi antenna [51] to the SDR. Due to the high self-interference problem, we cannot use the monostatic setup on LoREA, we simulate the equivalent path loss in monostatic configurations by keeping the carrier generator and the receiver equidistant from the tag while maximising the distance between them. We also operate LoREA in low bitrate mode. We program both the WISP and LoREA to transmit with the minimum possible delay. As a metric, we measure the achieved goodput.

Results. Figure 11 shows that as the distance between the WISP and the RFID reader increases, the achieved bitrate drops significantly. This is due to the SNR of the backscattered signal decreasing at the reader and approaching the sensitivity levels of the reader. We observe a maximum distance of approximately 17 m, which is consistent with the maximum advertised range of the Impinj Speedway R420 RFID reader [19].

LoREA on the other hand, achieves a similar good-

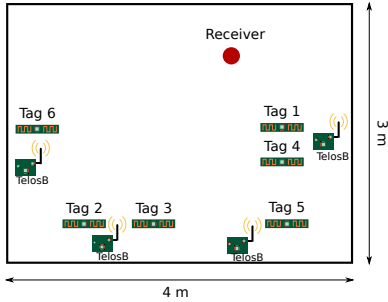


Figure 12: *Spatial setup for distributed-carrier setup.*

put but much higher range even in a somewhat less favourable configuration. To put the numbers in context, LOREA achieves a range, in bistatic mode, of approximately 225 m with the backscatter tag 1 m away, and 100 m with the backscatter tag 12 m away from the carrier generator at similar bitrates as the WISP. LOREA, in certain cases, achieves a range that is one order of magnitude longer compared to existing RFID readers. LOREA achieves a higher range in spite of the RFID reader using sub GHz frequency for communication, which offers better propagation characteristics.

The higher range achieved by LOREA is due to three reasons. First, LOREA shifts the weak backscattered signal away from the carrier which reduces the noise floor, thereby improving the SNR. Second, LOREA uses a radio which offers receiver sensitivity that is almost 20 dB higher (approximately -104 dBm) compared to the -84 dBm the R420 reader offers, a typical sensitivity for commercial RFID readers. Finally, most commercial RFID readers operate in a monostatic configuration which, as we have discussed in Section 3.3, limits the achievable range significantly.

4.3 Leveraging Carriers from Existing Infrastructure

Next, we perform an experiment to demonstrate how LOREA can leverage existing infrastructure to generate suitable carriers rather than relying on the reader to generate the carrier as RFID readers do. We deploy six MSP430-based backscatter tags in an office in close proximity to TelosB sensor nodes [38]. The tags periodically backscatter packets with random payloads. A LOREA reader is also placed in the room. The spatial setup of the experiment is shown in Fig. 12.

Experimental setup. We use the deployed TelosB sensor nodes for carrier generation. Their radio chips (CC2420) feature a test mode that allows to generate an unmodulated carrier at an output power of 0 dBm. We collect received packets over a time span of five hours.

Results. Fig. 13 shows the BER for each of the six backscatter tags. BERs are generally low, except for tag 2, which has the longest distance to the receiver. We attribute the bit errors that we observe to interference from other coexisting wireless networks and occasional collisions between transmissions from tags. We

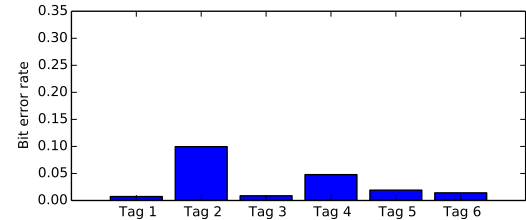


Figure 13: *Bit error rate for distributed-carrier setup.* LOREA can make use of several carriers from deployed infrastructure.

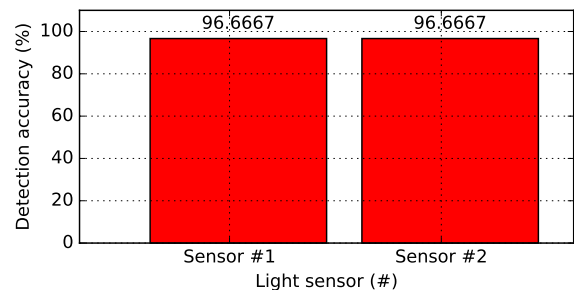


Figure 14: *Backscatter-based light sensor.* The LOREA-based system achieves a high detection accuracy.

do not observe distinct temporal variations in the bit error rate. We conclude that using several carriers simultaneously is feasible, and that slight offsets in the carrier frequency between carrier generators (which are inevitable due to variations in crystals) do not noticeably affect communication.

5. PROOF-OF-CONCEPT APPLICATIONS

In this section, we present two proof-of-concept applications realized using LOREA.

5.1 Passive Visible Light Markers

Since visible light is omnipresent indoors, it is attractive for sensing applications. Recent systems leverage visible light and shadows cast on light sensors to enable applications like gesture recognition [27, 26] and activity sensing [18, 62]. These systems, however, require the deployment of a large number of photodiodes on the floor or ceiling and extensive cabling of the light sensors. The requirement to physically connect the light sensors using wires often makes these systems rigid and difficult to use in actual deployments. Wireless light sensors could help. However, platforms based on active radios might require regular battery replacement.

Battery-free light sensors are attractive as such sensors could be embedded in walls or floors at the time of construction (with the light sensor itself exposed to the outside of the wall/floor) and left unattended. Backscatter is a prime candidate for providing wireless connectivity due to its ultra-low power nature. We

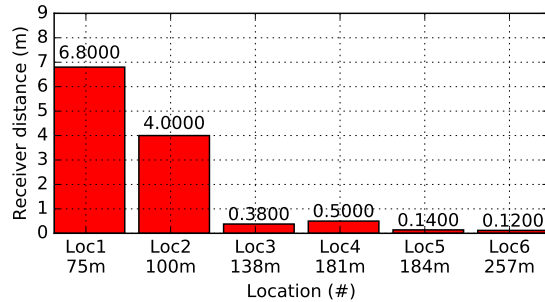


Figure 15: *Receiving backscatter transmissions in parking space.* The farther the tag is from the carrier generator, the closer the reader has to be to the tag to receive.

have earlier demonstrated a proof-of-concept battery-free light sensor to enable localization using the WISP 5.0 CRFID platform [10]. Our earlier system, however, suffered from the high cost of the reader ($\sim \$1600$), required three large antennas and achieved only a short communicate range. LoREA could help such applications by achieving a large range at very low cost.

We implement a proof-of-concept light sensor application using LoREA. We connect a photodiode to an MSP430-based backscatter tag ($\sim \$16$) and program it to backscatter light readings when a drop in the light intensity is detected. We generate the carrier signal using the test mode on the WiFi radio CC3200 ($\sim \$30$). Next, we position the sensor inside our offices, and position two receivers outside approximately 6 m and 9 m away from the sensor. The sensor and receivers are not in line of sight and are separated by walls in our office. We walk close to the light sensor such that the shadow falls on the photodiode. We obstruct the sensor 30 times at an interval of 60 s, and record at the receiver whether the event was received. We observe that both the receivers detect the shadow event with high accuracy of $\geq 96\%$. The entire setup costs less than \$100 and yet achieves a high performance.

5.2 Mobile Reader

Mobile backscatter readers can be useful for applications in, for example, libraries [41], offices of the future, and at manufacturing lines. However, existing backscatter readers are energy expensive and bulky which severely limits their usage on mobile platforms since their batteries need to be exchanged often. Due to its lower power consumption (see Table 2), LoREA enables such mobile applications.

One of the key elements that help to achieve a LoREA receiver’s low power consumption is the bistatic mode of operation, which decouples the energy-expensive carrier generation from the receiver. Decoupling the carrier generator, however, introduces a new challenge: tags demonstrate varied communication range, due to different distances from the carrier generator.

To demonstrate this problem, we distribute backscatter tags at six different locations in the parking space of the university campus. The backscatter tags are not in line of sight of the carrier generator. We find the maximum communication distance between the tag and the reader. Figure 15 demonstrates that the communication range is higher for tags closer to the carrier generator, while for tags far away the reader has to be close to the tag to receive transmissions.

In a concrete application scenario, one could deploy several carrier generators as shown in Section 4.3. Another option is to devise trajectories that allow the mobile reader to query the tags near the carrier generator from large distances and tags far away from the carrier generator from short distances. While we note that LoREA due to its low power consumption enables such mobile reader applications, we leave the open issues raised by this use case to future work.

6 RELATED WORK

This section begins with a summary of other efforts in designing low-power backscatter readers followed by an overview of CRFID platforms, we next discuss briefly self-interference mitigation and finally discuss recent backscatter systems.

Low power readers. There have been some prior attempts to develop low-cost backscatter readers. Braido is a backscatter reader that can switch between active and passive radios depending on the energy constraints of the host device [17]. Similar to our solution, Braido can function as a low-cost and low-power backscatter reader, but achieves a receiver range of 1.8 m at 100 kbps. As a comparison, LoREA can reach beyond 200 m due to three primary reasons: First, Braido uses passive receivers similar to the ones found on RFID tags resulting in a sensitivity of approximately -60 dBm. By contrast, the receivers employed by LoREA are off-the-shelf radio chips with a sensitivity as low as -104 dBm. Second, we separate the weak backscattered signal from the strong carrier helping to improve the the SNR. Finally, we enable bi-static operation of the reader which helps further reduce self-interference. Nikitin et al. aim to reduce the cost of the reader and presents a design of a simple and a low-cost reader for RFID applications [32] and achieve a range of only 15 cm.

CRFID platforms. WISP [55] and Moo [60] are computational RFID platforms that leverage backscatter communication and allow interfacing with sensors. They rely, however, on the use of traditional RFID readers inheriting also their limitations. Similar to our backscatter tag, these platforms use the MSP430. In future work we plan to make them interoperable with LoREA.

Self-interference mitigation. There has been significant recent work to reduce self-interference and enable full-duplex operations on radios [22, 9, 4]. These techniques, however, significantly increase the complexity,

power consumption and cost of the reader.

Liu et al. present a design to reduce self-interference and enable full-duplex operation on ambient backscatter devices [29]. These designs achieve only few meters of range. Recent backscatter systems leverage the spectral mixing property of backscatter transmissions to shift backscatter transmissions away from the carrier to reduce self-interference [24, 61, 11, 37, 36, 59]. We build upon these recent designs to develop an efficient reader for CRFID devices which achieves high communication range and low cost.

Ma et al. [30] use non-linear elements attached to the WISP platform to reduce self-interference and achieve accurate 3D localization. While Ma et al. [30] also reduce self-interference, we target a different problem: by shifting the carrier we reduce self-interference to lower the cost of the backscatter reader and enable higher communication ranges.

Passive backscatter. Passive transmissions of commodity radio protocols have recently attracted significant interest due to the ability to synthesize packets compatible with existing wireless standards like ZigBee [21, 36, 37], Bluetooth [11] and WiFi [21, 24, 61] with a power consumption that is three to four orders of magnitude lower than conventional radios. Ensworth et al. demonstrate the ability to synthesize BLE advertisements using backscatter communication [11]. Kellogg et al. synthesize WiFi packets using backscatter. Further, they demonstrate that an ASIC implementation of the radio would consume only $14.5 \mu W$ [24]. Iyer et al. improve upon this work and demonstrate the ability to backscatter WiFi and ZigBee packets using transmissions generated from a BLE radio [21].

While these works do not need a separate backscatter reader and can use off-the-shelf devices like smartphones as a receiver, they are still constrained. First, the intricacies of implementing complex protocols such as WiFi or ZigBee require these devices to implement the baseband logic on an FPGA which can consume power in the same order as conventional radio chips. Implementing on ICs might reduce the power consumption [24], however, to the best of our knowledge such commercial implementation are not easily available. Fabricating custom ICs can be prohibitively expensive, especially for small quantities, making them inaccessible to the wider research community. Second, existing wireless protocols operate at high bitrates, and the receiver sensitivity decreases with increasing bitrates reducing achievable range. For example, improved sensitivity due to operations at low bitrates enables LOREA achieve $7 \times$ larger range as compared to Passive WiFi [24].

Ambient backscatter. Ambient backscatter leverages radio signals such as TV transmissions [28] or WiFi traffic [3, 23, 61] to dispense with the need for an external reader or a device to generate the external carrier. Parks et al. demonstrate passive tag-to-tag communication using ambient TV signals [28]. They further

improve on the design to enable through-the-wall operations and achieve high throughput [35]. Ambient backscatter using TV signals, however, is limited to operate only in the vicinity of TV towers where the signal is strong enough (approx. -30 dBm) taking it out of reach for many deployments. Furthermore, the communication range is limited to about 30 m [35].

WiFi backscatter. Recent attempts leverage ambient WiFi signals to enable backscatter communication. Kellogg et al. demonstrate the feasibility of backscattering WiFi signals and receiving on commodity smart phones [23]. They achieve only a short range of 2.1 m at a throughput of 1 kbps due to severe self-interference. Zhang et al. improve upon WiFi backscatter, and using frequency-shifting to separate backscattered signals from WiFi packet transmissions reduce self-interference and achieve a range of 4.8 m. Bharadia et al. demonstrate high throughput backscatter (around 1 Mbps) with distances upto 5 m [3]. Their design uses extensive self-interference cancellation techniques at the receiver making the system both complex and expensive. HitchHike [61] enables communication between commodity WiFi radios by changing codewords of WiFi transmissions and achieve a range of 54 m. The HitchHike tag is based on an FPGA due to the need for precise timing to change the phase of symbols in WiFi packets. While these approaches avoid the need for a dedicated device to generate an unmodulated carrier signal, they, as noted by Iyer et al. [21] need large amount of WiFi packets to be sent which can occupy almost half of the available spectrum. Hence, they could further aggravate the problem of Cross Technology Interference (CTI). LOREA, on the other hand allows commodity radios to generate a carrier and occupies only 4 MHz of the spectrum, less than channel bandwidth of ZigBee, easing coexistence with other wireless networks.

7. CONCLUSIONS

In this paper we have presented LOREA, a new architecture for the next-generation backscatter readers. LOREA departs from previous designs in that it avoids the need for complex and expensive self-interference: LOREA separates the backscatter transmissions from the carrier by shifting the weak backscattered signal away from the carrier signal. Furthermore, LOREA decouples carrier generation from data reception which enables other devices such as sensor nodes and smartphones to generate the carrier, which improves range and scalability. In LOREA, receivers are cheap off-the-shelf radios with high sensitivity which leads to costs that are about one magnitude below that of commercial RFID readers. Putting these techniques together makes LOREA a low-cost but very efficient backscatter reader that achieves a range beyond 200 m in line of sight, outperforming state-of-the-art solutions.

8. REFERENCES

[1] Analog Devices. HMC190BMS8. Accessed: 02-09-2016. <http://www.analog.com/media/en/technical-documentation/data-sheets/hmc190b.pdf>.

[2] Beaglebone black. Accessed: 02-09-2016. <https://beagleboard.org>.

[3] D. Bharadia, K. R. Joshi, M. Kotaru, and S. Katti. Backfi: High throughput wifi backscatter. In *Proceedings of the 2015 ACM Conference on Special Interest Group on Data Communication*, SIGCOMM '15, pages 283–296, New York, NY, USA, 2015. ACM.

[4] D. Bharadia and S. Katti. Full duplex mimo radios. In *Proceedings of the 11th USENIX Conference on Networked Systems Design and Implementation*, NSDI'14, pages 359–372, Berkeley, CA, USA, 2014. USENIX Association.

[5] N. A. Bhatti, M. H. Alizai, A. A. Syed, and L. Mottola. Energy harvesting and wireless transfer in sensor network applications: Concepts and experiences. *ACM Trans. Sen. Netw.*, 12(3):24:1–24:40, Aug. 2016.

[6] M. Buettner, B. Greenstein, and D. Wetherall. Dewdrop: An energy-aware runtime for computational rfid. In *Proceedings of the 8th USENIX Conference on Networked Systems Design and Implementation*, NSDI'11, pages 197–210, Berkeley, CA, USA, 2011. USENIX Association.

[7] M. Buettner, R. Prasad, M. Philipose, and D. Wetherall. Recognizing daily activities with rfid-based sensors. In *Proceedings of the 11th International Conference on Ubiquitous Computing*, UbiComp '09, pages 51–60, New York, NY, USA, 2009. ACM.

[8] M. Buettner and D. Wetherall. A software radio-based UHF RFID reader for PHY/MAC experimentation. In *2011 IEEE International Conference on RFID*, pages 134–141, Apr. 2011.

[9] J. I. Choi, M. Jain, K. Srinivasan, P. Levis, and S. Katti. Achieving single channel, full duplex wireless communication. In *Proceedings of the Sixteenth Annual International Conference on Mobile Computing and Networking*, MobiCom '10, pages 1–12, New York, NY, USA, 2010. ACM.

[10] E. Di Lascio, A. Varshney, T. Voigt, and C. Pérez-Penichet. Localight: A battery-free passive localization system using visible light: Poster abstract. In *Proceedings of the 15th International Conference on Information Processing in Sensor Networks*, IPSN '16, pages 60:1–60:2, Piscataway, NJ, USA, 2016. IEEE Press.

[11] J. F. Ensworth and M. S. Reynolds. Every smart phone is a backscatter reader: Modulated backscatter compatibility with bluetooth 4.0 low energy (ble) devices. In *2015 IEEE International Conference on RFID (RFID)*, pages 78–85, April 2015.

[12] EPC GEN 2. Accessed: 02-09-2016. <http://www.gs1.org/epcrfid/epc-rfid-uhf-air-interface-protocol/2-0-1>.

[13] Ettus Research. USRP B200. Accessed: 02-09-2016. <https://www.ettus.com/product/details/UB200-KIT>.

[14] J. Gummesson, S. S. Clark, K. Fu, and D. Ganesan. On the limits of effective hybrid micro-energy harvesting on mobile rfid sensors. In *Proceedings of the 8th International Conference on Mobile Systems, Applications, and Services*, MobiSys '10, pages 195–208, New York, NY, USA, 2010. ACM.

[15] J. Gummesson, P. Zhang, and D. Ganesan. Flit: A bulk transmission protocol for rfid-scale sensors. In *Proceedings of the 10th International Conference on Mobile Systems, Applications, and Services*, MobiSys '12, pages 71–84, New York, NY, USA, 2012. ACM.

[16] P. Hu, P. Zhang, and D. Ganesan. Laissez-faire: Fully asymmetric backscatter communication. In *Proceedings of the 2015 ACM Conference on Special Interest Group on Data Communication*, SIGCOMM '15, pages 255–267, New York, NY, USA, 2015. ACM.

[17] P. Hu, P. Zhang, M. Rostami, and D. Ganesan. Braidio: An integrated active-passive radio for mobile devices with asymmetric energy budgets. In *Proceedings of the 2016 Conference on ACM SIGCOMM 2016 Conference*, SIGCOMM '16, pages 384–397, New York, NY, USA, 2016. ACM.

[18] M. Ibrahim, V. Nguyen, S. Rupavatharam, M. Jawahar, M. Gruteser, and R. Howard. Visible light based activity sensing using ceiling photosensors. In *Proceedings of the 3rd Workshop on Visible Light Communication Systems*, VLCS '16, pages 43–48, New York, NY, USA, 2016. ACM.

[19] Impinj. Impinj speedway r420. 2016.

[20] Impinj R2000 RFID Reader Chip. Accessed: 02-10-2016.

[21] V. Iyer, V. Talla, B. Kellogg, S. Gollakota, and J. Smith. Inter-technology backscatter: Towards internet connectivity for implanted devices. In *Proceedings of the 2016 Conference on ACM SIGCOMM 2016 Conference*, SIGCOMM '16, pages 356–369, New York, NY, USA, 2016. ACM.

[22] M. Jain, J. I. Choi, T. Kim, D. Bharadia, S. Seth, K. Srinivasan, P. Levis, S. Katti, and P. Sinha. Practical, real-time, full duplex wireless. In *Proceedings of the 17th Annual International Conference on Mobile Computing and Networking*,

MobiCom '11, pages 301–312, New York, NY, USA, 2011. ACM.

[23] B. Kellogg, A. Parks, S. Gollakota, J. R. Smith, and D. Wetherall. Wi-fi backscatter: Internet connectivity for rf-powered devices. In *Proceedings of the 2014 ACM Conference on SIGCOMM*, SIGCOMM '14, pages 607–618, New York, NY, USA, 2014. ACM.

[24] B. Kellogg, V. Talla, S. Gollakota, and J. R. Smith. Passive wi-fi: Bringing low power to wi-fi transmissions. In *13th USENIX Symposium on Networked Systems Design and Implementation (NSDI 16)*, pages 151–164, Santa Clara, CA, Mar. 2016. USENIX Association.

[25] J. Kimionis et al. Increased Range Bistatic Scatter Radio. *IEEE Transactions on Communications*, 62(3):1091–1104, Mar. 2014.

[26] T. Li, C. An, Z. Tian, A. T. Campbell, and X. Zhou. Human sensing using visible light communication. In *Proceedings of the 21st Annual International Conference on Mobile Computing and Networking*, MobiCom '15, pages 331–344, New York, NY, USA, 2015. ACM.

[27] T. Li, Q. Liu, and X. Zhou. Practical human sensing in the light. In *Proceedings of the 14th Annual International Conference on Mobile Systems, Applications, and Services*, MobiSys '16, pages 71–84, New York, NY, USA, 2016. ACM.

[28] V. Liu, A. Parks, V. Talla, S. Gollakota, D. Wetherall, and J. R. Smith. Ambient backscatter: Wireless communication out of thin air. In *Proceedings of the ACM SIGCOMM 2013 Conference on SIGCOMM*, SIGCOMM '13, pages 39–50, New York, NY, USA, 2013. ACM.

[29] V. Liu, V. Talla, and S. Gollakota. Enabling instantaneous feedback with full-duplex backscatter. In *Proceedings of the 20th Annual International Conference on Mobile Computing and Networking*, MobiCom '14, pages 67–78, New York, NY, USA, 2014. ACM.

[30] Y. Ma, X. Hui, and E. C. Kan. 3d real-time indoor localization via broadband nonlinear backscatter in passive devices with centimeter precision. In *Proceedings of the 22Nd Annual International Conference on Mobile Computing and Networking*, MobiCom '16, pages 216–229, New York, NY, USA, 2016. ACM.

[31] S. Naderiparizi, A. N. Parks, Z. Kapetanovic, B. Ransford, and J. R. Smith. Wispcam: A battery-free rfid camera. In *2015 IEEE International Conference on RFID (RFID)*, pages 166–173, April 2015.

[32] P. V. Nikitin, S. Ramamurthy, and R. Martinez. Simple low cost uhf rfid reader. In *Proc. IEEE Int. Conf. RFID*, pages 126–127, 2013.

[33] P. V. Nikitin and K. V. S. Rao. Antennas and propagation in uhf rfid systems. In *2008 IEEE International Conference on RFID*, pages 277–288, April 2008.

[34] F. J. Oppermann et al. A decade of wireless sensing applications: Survey and taxonomy. In *The Art of Wireless Sensor Networks*, pages 11–50. Springer, 2014.

[35] A. N. Parks, A. Liu, S. Gollakota, and J. R. Smith. Turbocharging ambient backscatter communication. In *Proceedings of the 2014 ACM Conference on SIGCOMM*, SIGCOMM '14, pages 619–630, New York, NY, USA, 2014. ACM.

[36] C. Pérez-Penichet, F. Hermans, A. Varshney, and T. Voigt. Augmenting iot networks with backscatter-enabled passive sensor tags. In *Proceedings of the 3rd Workshop on Hot Topics in Wireless*, HotWireless '16, pages 23–27, New York, NY, USA, 2016. ACM.

[37] C. Pérez-Penichet, F. Hermans, A. Varshney, and T. Voigt. Passive sensor tags: Demo. In *Proceedings of the 22Nd Annual International Conference on Mobile Computing and Networking*, MobiCom '16, pages 477–478, New York, NY, USA, 2016. ACM.

[38] J. Polastre, R. Szewczyk, and D. Culler. Telos: Enabling ultra-low power wireless research. In *Proceedings of the 4th International Symposium on Information Processing in Sensor Networks*, IPSN '05, Piscataway, NJ, USA, 2005. IEEE Press.

[39] T. S. Rappaport. *Wireless Communications: Principles and Practice*. Prentice Hall, 2nd edition, 2002.

[40] A. P. Sample et al. Photovoltaic enhanced uhf rfid tag antennas for dual purpose energy harvesting. In *IEEE RFID 2011*.

[41] L. Shangguan and K. Jamieson. The design and implementation of a mobile rfid tag sorting robot. In *Proceedings of the 14th Annual International Conference on Mobile Systems, Applications, and Services*, MobiSys '16, pages 31–42, New York, NY, USA, 2016. ACM.

[42] J. R. Smith et al. A wirelessly-powered platform for sensing and computation. In *International Conference on Ubiquitous Computing*, 2006.

[43] J. R. Smith et al. A wirelessly-powered platform for sensing and computation. In *International Conference on Ubiquitous Computing*, pages 495–506. Springer, 2006.

[44] V. Talla, B. Kellogg, B. Ransford, S. Naderiparizi, S. Gollakota, and J. R. Smith. Powering the next billion devices with wi-fi. *arXiv preprint arXiv:1505.06815*, 2015.

[45] Texas Instruments. MSP430 FR5969. <http://www.ti.com/product/MSP430FR5969>.

[46] Texas Instruments. CC1310. Accessed: 02-09-2016.

http://www.ti.com/lit/ds/symlink/cc1310.pdf.

[47] Texas Instruments. CC2500. Accessed: 02-09-2016.
http://www.ti.com/lit/ds/symlink/cc2500.pdf.

[48] Texas Instruments. CC3200 launchpad. Accessed: 02-09-2016.
http://www.ti.com/tool/cc3200-launchxl.

[49] S. J. Thomas et al. Rich-media tags: Battery-free wireless multichannel digital audio and image transmission with uhf rfid techniques. In *IEEE RFID 2013*.

[50] TP-Link. TL-ANT2408CL.

[51] TP-Link. TL-ANT2409A.

[52] M. Tubaishat and S. Madria. Sensor networks: an overview. *IEEE Potentials*, 22(2):20–23, April 2003.

[53] A. Varshney, L. Mottola, M. Carlsson, and T. Voigt. Directional transmissions and receptions for high-throughput bulk forwarding in wireless sensor networks. In *Proceedings of the 13th ACM Conference on Embedded Networked Sensor Systems*, SenSys '15, pages 351–364, New York, NY, USA, 2015. ACM.

[54] J. Wang, H. Hassanieh, D. Katabi, and P. Indyk. Efficient and reliable low-power backscatter networks. In *Proceedings of the ACM SIGCOMM 2012 Conference on Applications, Technologies, Architectures, and Protocols for Computer Communication*, SIGCOMM '12, pages 61–72, New York, NY, USA, 2012. ACM.

[55] WISP 5.0. Accessed: 02-09-2016.
http://wisp5.wikispaces.com/WISP+Home.

[56] D. J. Yeager et al. Neuralwisp: A wirelessly powered neural interface with 1-m range. *IEEE Transactions on Biomedical Circuits and Systems*, 2009.

[57] P. Zhang and D. Ganesan. Enabling bit-by-bit backscatter communication in severe energy harvesting environments. In *Proceedings of the 11th USENIX Conference on Networked Systems Design and Implementation*, NSDI'14, pages 345–357, Berkeley, CA, USA, 2014. USENIX Association.

[58] P. Zhang, P. Hu, V. Pasikanti, and D. Ganesan. Ekhonet: High speed ultra low-power backscatter for next generation sensors. In *Proceedings of the 20th Annual International Conference on Mobile Computing and Networking*, MobiCom '14, pages 557–568, New York, NY, USA, 2014. ACM.

[59] P. Zhang, M. Rostami, P. Hu, and D. Ganesan. Enabling practical backscatter communication for on-body sensors. In *Proceedings of the 2016 Conference on ACM SIGCOMM 2016 Conference*, SIGCOMM '16, pages 370–383, New York, NY, USA, 2016. ACM.

[60] H. Zhang et al. Moo: A batteryless computational rfid and sensing platform. 2011.

[61] P. Zhang et al. Hitchhike: Practical backscatter using commodity wifi. In *ACM SENSYS 2016*.

[62] X. Zhou and A. T. Campbell. Visible light networking and sensing. In *Proceedings of the 1st ACM Workshop on Hot Topics in Wireless*, HotWireless '14, pages 55–60, New York, NY, USA, 2014. ACM.